Electronic Supplementary Information

An Anthracenecarboximide-Guanidine Based Fluorescent Probe for Selective Detection of Glyoxals at Weak Acidic Condition

Junwei Chen,[a,#] Yuna Lin,[a,#] Wanjin Xing,[a] Xingchen Zhang,[a] Huan Xu,[a,*] Wei Wang,[b,*] and Kaiyan Lou[a,*]

[a] State Key Laboratory of Bioreactor Engineering, Shanghai Frontiers Science Center of Optogenetic Techniques for Cell Metabolism, Shanghai Key Laboratory of New Drug Design, and Shanghai Key Laboratory of Chemical Biology, School of Pharmacy, East China University of Science & Technology, 130 Meilong Road, Shanghai 200237, China.
[b] Department of Pharmacology and Toxicology and BIO5 Institute, University of Arizona, Tucson, AZ 85721-0207, USA.

Table of Contents

General Information

Commercial reagents were purchased from commercial suppliers and used as received, unless otherwise stated. Manuka honey (brand name "nzgolhealth" with UMF values 10+ and 20+ were purchased from www.jd.com. Acacia honey was friendly donated by a local bee farmer in Anhui province, China.

^{1}H and ^{13}C NMR spectra were recorded on Bruke DRX 400 (400 MHz). Data for ^{1}H are reported as follows: chemical shift (ppm), and multiplicity (s = singlet, bs = broad singlet, d = doublet, t = triplet, q = quartet, m = multiplet). Data for ^{13}C NMR are reported as ppm. Mass Spectra were obtained from East China University of Science and Technology LC-Mass spectral facility. UV-Vis spectra were collected on a Shimadzu UV-1800 spectrophotometer. Fluorescence spectra were collected on a FluoroMax-4 (Horiba Scientific) fluorescence spectrophotometer with slit widths were set at 4 nm both for excitation and emission unless otherwise stated. The pH measurements were carried out with a FE20 plus (Mettler Toledo) pH meter.

Part I Synthetic Procedures and Structural Characterizations:

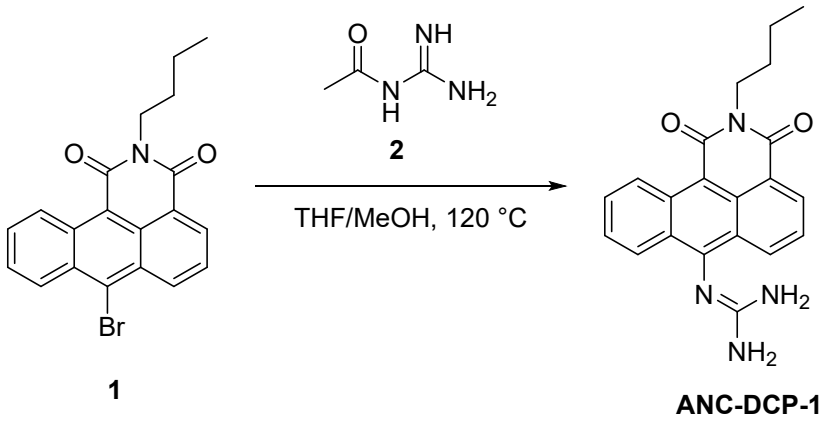

Scheme S1 Synthesis of the probe **ANC-DCP-1**

2-(*N*-butyl-anthracene-1,9-dicarboximide-10-yl)guanidine (ANC-DCP-1)

To a suspension of *N*-butyl-anthracene-10-bromide-1,9-dicarboximide **1**[1] (114 mg, 0.3 mmol) in 18 mL THF, was slowly added a solution of acetylguanidine **2** (152 mg, 1.5 mmol) in 3 mL methanol. The mixture was stirred in a sealed tube at 120 °C for overnight, and cooled to room temperature. Solvent was removed by a rotavapor. The residue was added 50 mL water and extracted with methylene chloride (50 mL ×3). The organic layer was combined and washed with brine, dried over anhydrous magnesium sulfate, filtered and concentrated. The crude product was purified by silica gel column chromatographyusing CH_2Cl_2/MeOH (10:1, v/v) as eluent to afford the probe **ANC-DCP-1** (84 mg, 78% yield) as purple solid. ^{1}H NMR (DMSO-d_6, 400 MHz) δ 9.95 (d, J = 9.0 Hz, 1H), 8.62 (d, J = 7.0 Hz, 1H), 8.54 (d, J = 8.4 Hz, 1H), 8.32 (d, J = 8.6 Hz, 1H), 7.81 (t, J = 7.8 Hz, 1H), 7.70 (t, J = 7.8 Hz, 1H), 7.57 (t, J =7.6 Hz, 1H), 6.39 (s, 4H), 4.15 (t, J = 6.8 Hz, 2H), 1.65 (p, J = 7.6 Hz, 2H), 1.38 (sixtet, J = 7.5 Hz, 2H), 0.95 (t, J = 7.3 Hz, 3H); ^{13}C NMR (400 MHz, DMSO-d_6) δ 163.8, 163.2, 158.9, 154.4, 135.5, 133.3, 133.3, 131.1, 130.3, 126.9, 126.0, 125.3, 123.7, 122.4, 122.0, 121.5, 103.1, 39.0, 29.9, 19.9, 13.8; ESI-HRMS: m/z $[M+H]^+$ calcd for $C_{21}H_{20}N_4O_2$ 361.1659, found 361.1666.

Part II: Additional Fluorescence and Absorption Spectroscopy Studies

2.1 Spectroscopic materials

All aqueous solutions were prepared using double distilled water. **ANC-DCP-1** stock solution (1 mM in dry DMSO) was prepared and stored at -20 °C. All fluorescence and absorption spectroscopic measurements were performed in 10 mM phosphate solution at pH 6.0 at 25 °C unless otherwise stated.

Samples for absorption and fluorescence measurements were contained in 1 cm×1 cm quartz cuvettes (3.5 mL volume).

2.2 pH-dependent absorption spectra of ANC-DCP-1 and its pKa.

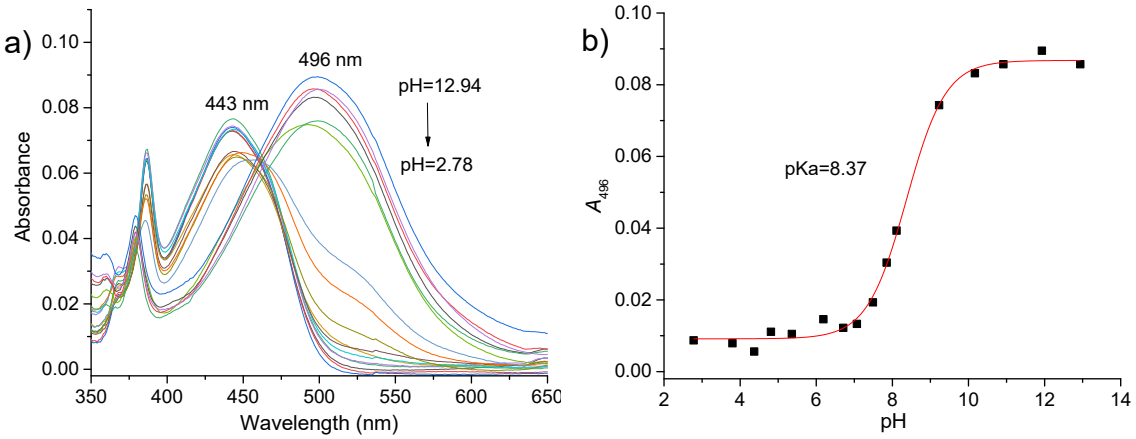

Figure S1 a) pH-dependent absorption spectra of **ANC-DCP-1** (10 μM) at various pKas; b) pKa calculation based on non-linear fitting of the curve of measured absorbance at 496 versus the corresponding pH value.

2.3 The absorption spectra of ANC-DCP-1 upon addition of 200 equiv. MGO at pH 7.4 and 5.0.

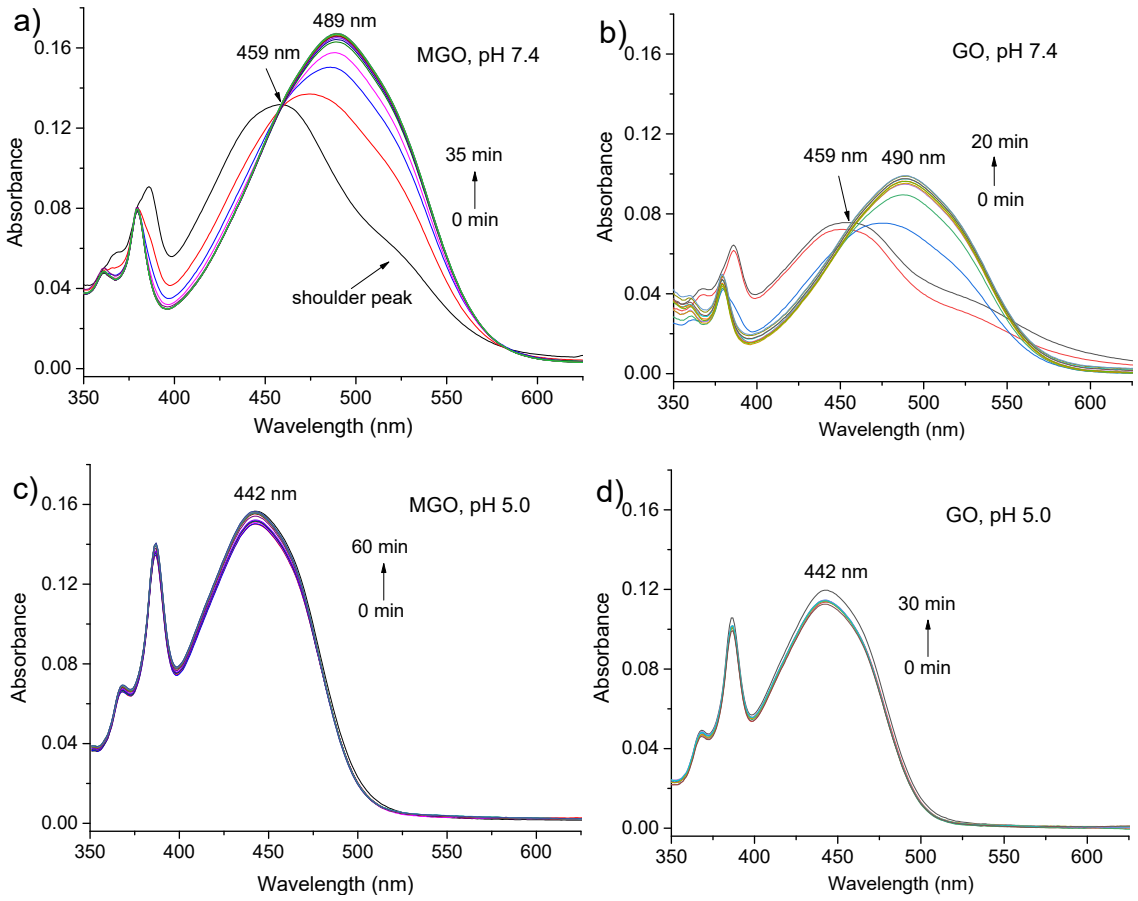

Figure S2 a-b) Time-dependent UV-Vis spectra of **ANC-DCP-1** (20 μM) upon additio n of 200 equiv. MGO (a) and 200 equiv. GO (b) at pH 7.4; c-d) Time-dependent UV-Vis spectra of **ANC-DCP-1** (20 μM) upon addition of 200 equiv. MGO (c) or 200 equiv. GO (d) at pH 5.0.

2.4 pH-dependent (pH 5.0 to 7.5) fluorescence intensity studies of ANC-DCP-1 incubation with 200 equiv. MGO or GO for 2h.

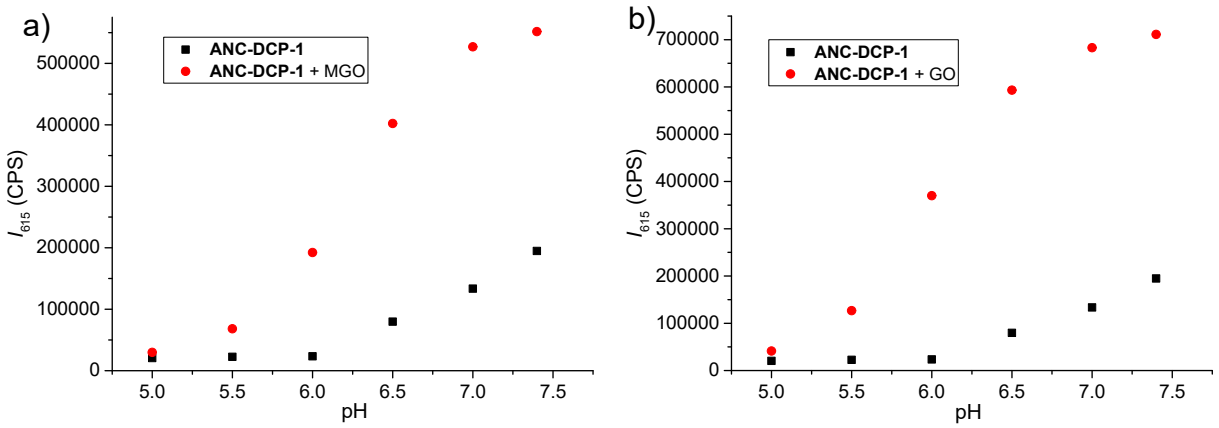

Figure S3 pH-dependent fluorescence intensity at 615 nm (λ_{ex} = 525 nm) for **ANC-DCP-1** (5 μM) after incubation with 200 equiv. of MGO (a) or GO (b) at various pHs from 5.0-7.4. The incubation time was 1 h for MGO and 2 h for GO.

2.5 Normalized fluorescence excitation and emission spectra of ANC-DCP-1 before and after addition of 200 equiv. MGO or GO at pH 6.0.

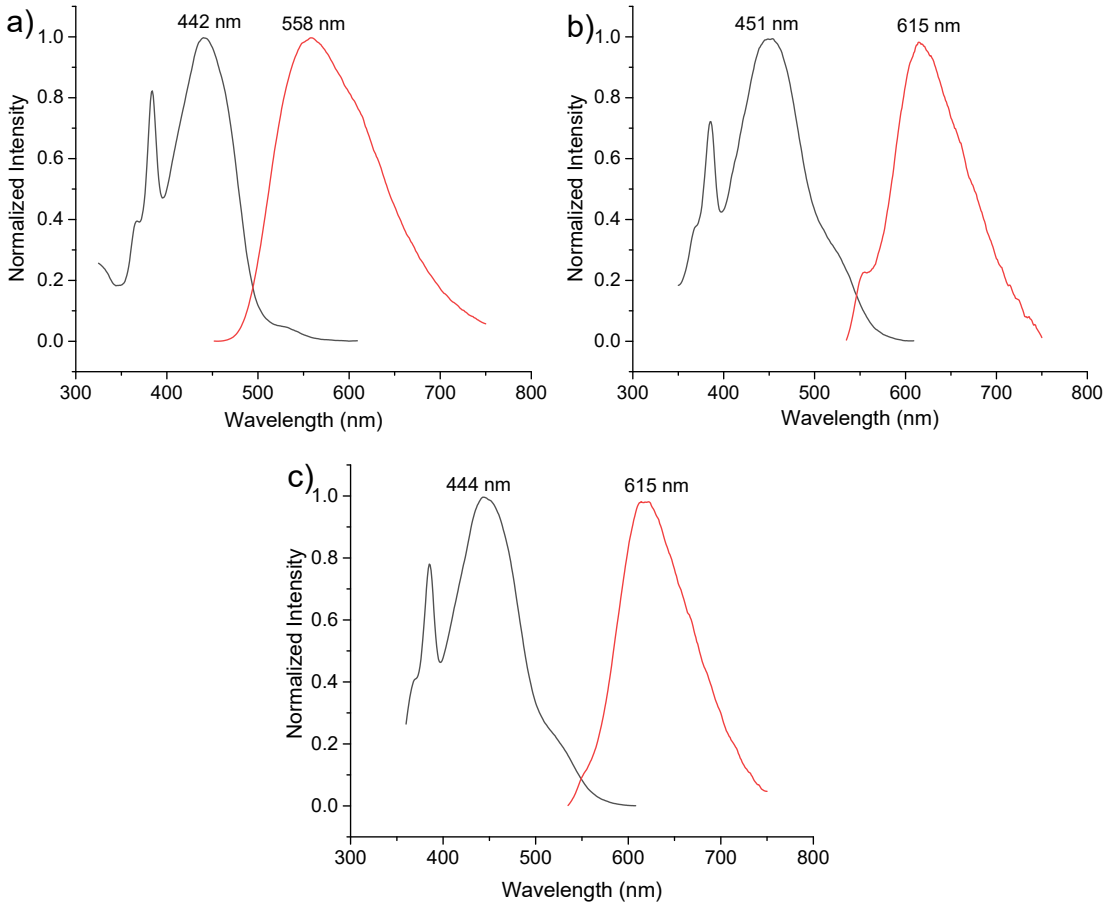

Figure S4 a) Normalized fluorescence excitation (λ_{em} = 558 nm) and emission spectra (λ_{ex} = 442 nm) of the probe **ANC-DCP-1** (5 μM) in pH 6.0 PBS buffer; b) Normalized fluorescence excitation (λ_{ex} =

615 nm) and emission spectra (λ_{ex} = 451 nm) of the probe **ANC-DCP-1** (5 μM) upon incubation with 200 equiv. MGO for 1 h in pH 6.0 PBS buffer; c) Normalized fluorescence excitation (λ_{ex} = 615 nm) and emission spectra (λ_{ex} = 444 nm) of the probe **ANC-DCP-1** (5 μM) upon incubation with 200 equiv. MGO for 1 h in pH 6.0 PBS buffer.

2.6 Time-dependent fluorescence emission studies of ANC-DCP-1 in response to 200 equiv. MGO or GO at pH 6.0.

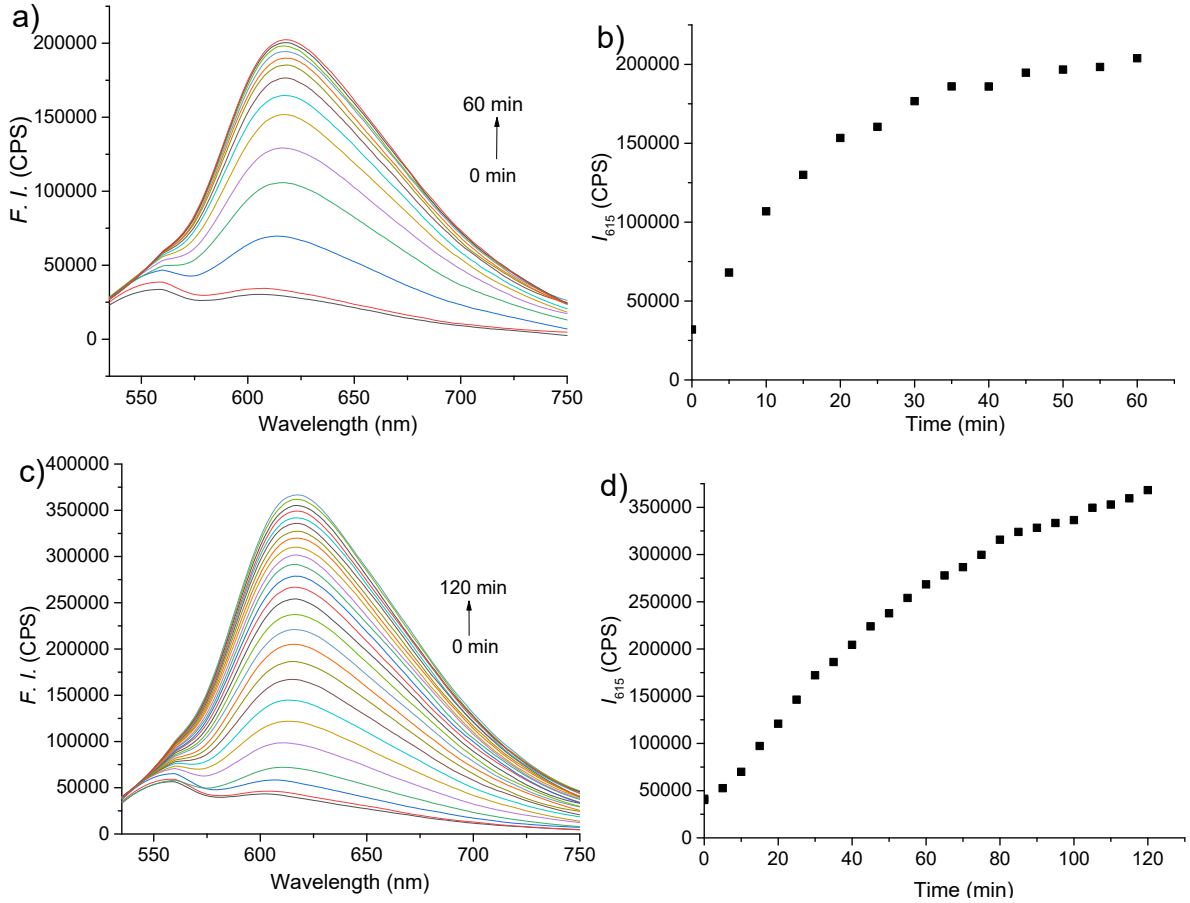

Figure S5 a) Time-dependent fluorescence emission spectra of the probe **ANC-DCP-1** (5 μM) upon addition 200 equiv. of MGO; b) Time-dependent fluorescence intensity at 615 nm of the probe **ANC-DCP-1** (5 μM) upon addition 200 equiv. of MGO; c) Time-dependent fluorescence emission spectra of the probe **ANC-DCP-1** (5 μM) upon addition 200 equiv. of GO; d) Time-dependent fluorescence intensity at 615 nm of the probe **ANC-DCP-1** (5 μM) upon addition 200 equiv. of GO. (All measurement was taken at λ_{ex} = 525 nm in 10 mM PBS solution (pH 6.0) with slit = 3/3 nm at 37 °C)

2.7 Concentration-dependent fluorescence emission studies of ANC-DCP-1 upon incubation with 200 equiv. MGO or GO at pH 6.0 for 2 h.

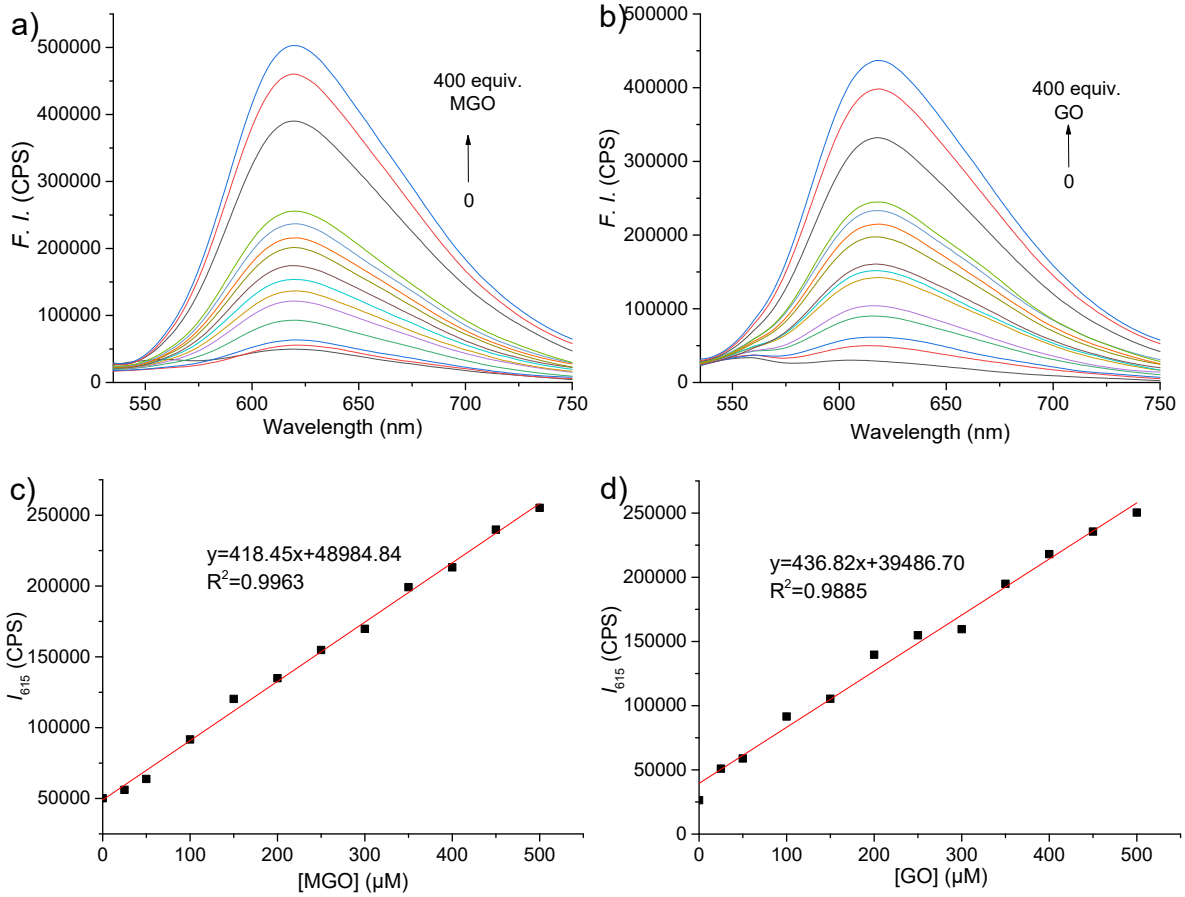

Figure S6 a-b) Concentration-dependent fluorescence emission spectra (λ_{ex}=525 nm) of the probe **ANC-DCP-1** (5 μM) incubated with 0-400 equiv. MGO (a) or GO (b) for 2 h; c-d) Linear regression of fluorescence intensity at 615 nm (λ_{ex}=525 nm) of the probe **ANC-DCP-1** (5 μM) versus the concentrations (0-500 μM) of MGO (c) or GO (d) incubated for 2h. The detection limit (S/N=3) were calculated as 12.6 and 12.1 μM for MGO and GO respectively.

2.8 Reversibility studies of the turn-on response of the probe ANC-DCP-1 for GOS

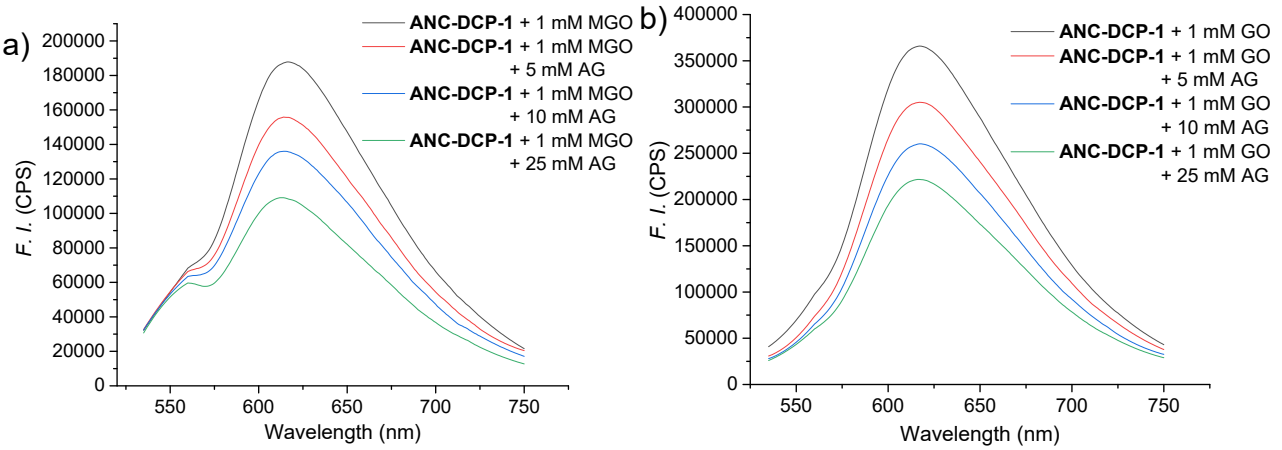

Figure S7 a) Concentration-dependent fluorescence emission spectra (λ_{ex} = 525 nm) of the probe **ANC-DCP-1** (5 μM) preincubated with 200 μM MGO in PBS buffer (10 mM, pH = 7.4) for 60 min and then incubated with different amounts (5, 10, 25 mM) of amino-guanidine (AG) for 30 min; b) Concentration-dependent fluorescence emission spectra (λ_{ex} = 525 nm) of the probe **ANC-DCP-1** (5 μM) preincubated with 200 μM GO in PBS buffer (10 mM, pH = 7.4) for 120 min and then incubated with different amounts (5, 10, 25 mM) of amino-guanidine (AG) for 30 min.

2.9 Time-dependent absorption spectra of ANC-DCP-1 upon incubation with 200 equiv. FA.

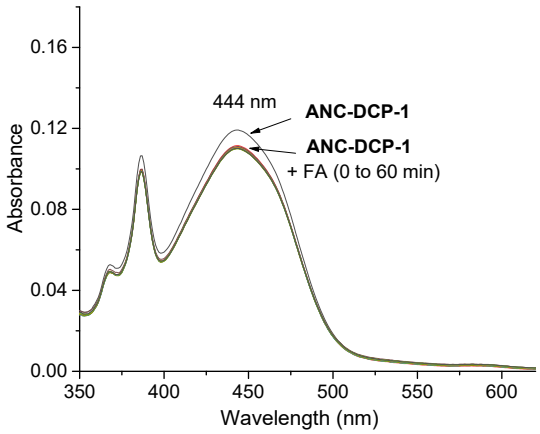

Figure S8 Time-dependent UV-Vis spectra of **ANC-DCP-1** (20 μM) upon addition of 200 equiv. FA.

Part III: Theoretical Calculations

All theoretical calculations [density functional theory (DFT) and the time-dependent DFT (TD-DFT)] were carried out using Gaussian 09 software.[2] The model probe **4** with *N*-methyl group instead of the *N*-butyl group in **ANC-DCP-1** and its GO adduct, *trans*-dihydroxyimidazolidine **6**, and their protonated forms **3** and **5** were used for calculations. All the compounds were optimized using DFT with B3LYP functional and 6-31+G (d, p) basis set (considered as in gas phase). The excited state related calculations were carried out with the TD-DFT, based on the optimized structure of the ground state. There are no imaginary frequencies in all calculated structures during the frequency analysis.

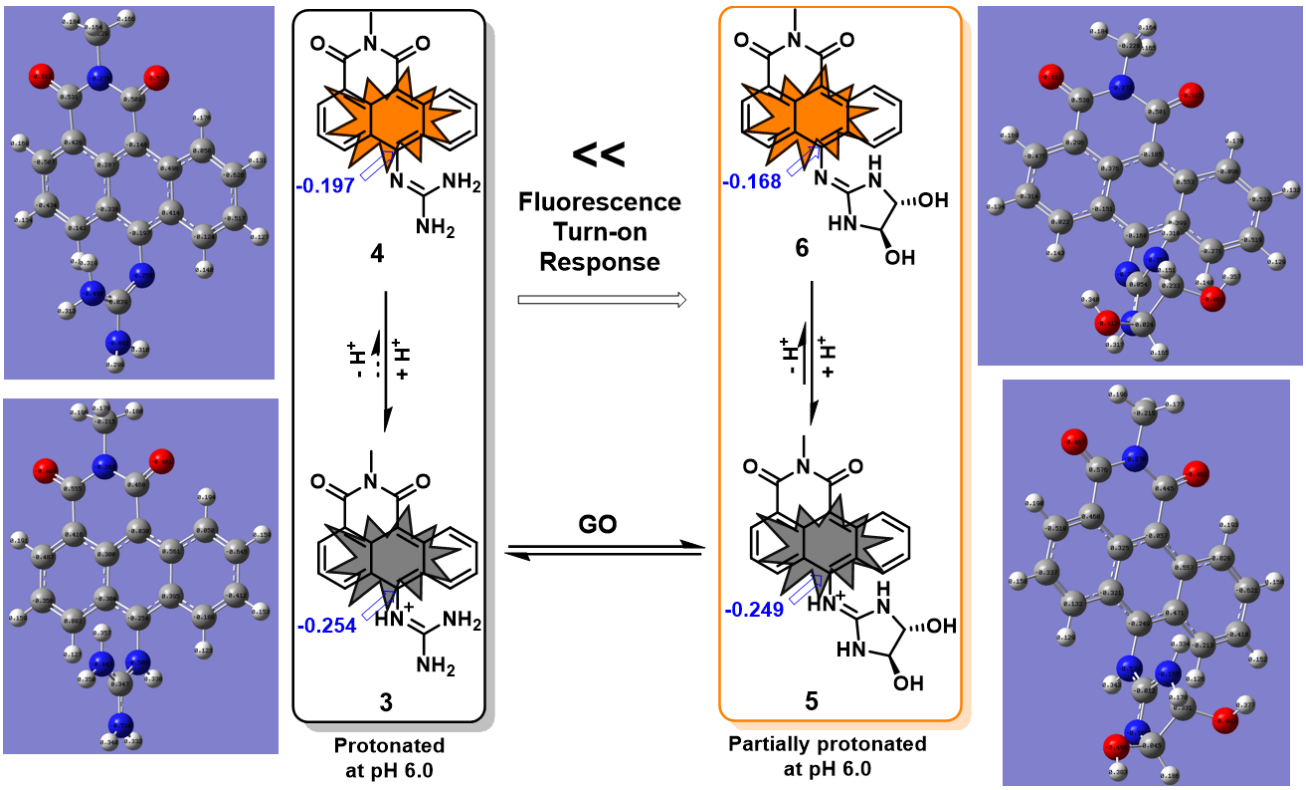

Figure S9 Structure of model compounds used in DFT calculations. The calculated Mulliken charge distributions on the 10-position of the ANC fluorophore were given.

(Fluorescence turn-on response can be explained as the following: 1) both the deprotonated species (**4** and **6**) have red-shifted absorption compared with protonated species (**3** and **5**) due to increased electron-donating at the 10-position and push-pull characteristic of the fluorophore; 2) the absorption wavelength difference allows selectively excite the red-shifted deprotonated species **4** and **6** in the reaction mixture; 3) at pH 6.0, almost all the probe is in the protonated form **3** while significant amount of **6** is in equilibrium with **5**; 4) the formation of the deprotonated species **6** and selective excitation of **6** is responsible for the fluorescence turn-on responses.)

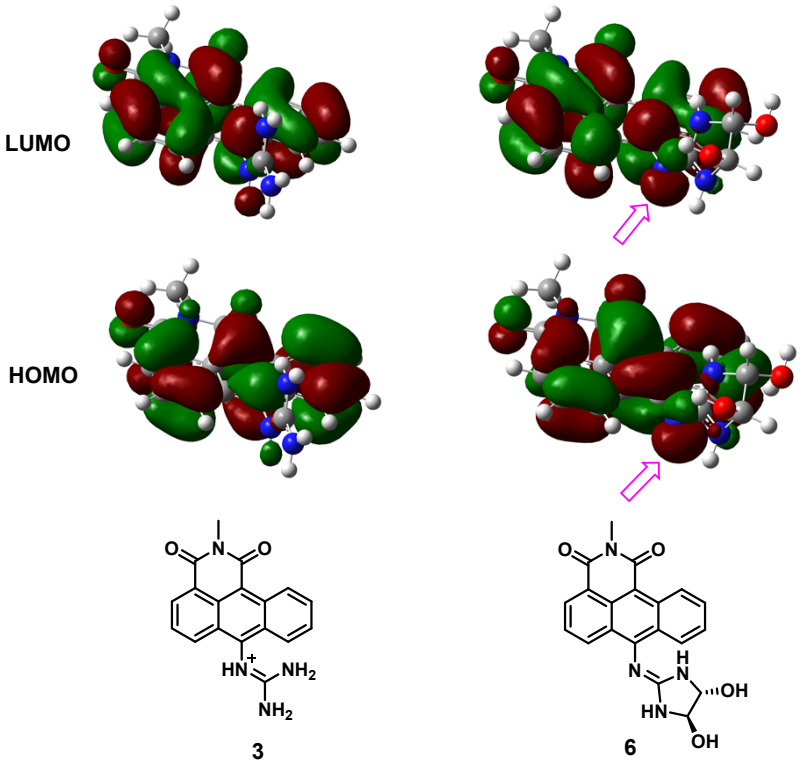

Figure S10 Calculated shape of HOMO and LUMO orbitals of the protonated probe **3** (the predominating specie at pH 6.0) and the deprotonated adduct **6** (the fluorescent specie at 6.0). (Significant p-π conjugation between the N atom of the guanidino- group directly connected to the fluorophore and the fluorophore is only found on the adduct **6** as pointed out by pink arrow)

Table S1 Electronic excitation energies (eV) and corresponding oscillator strengths (*f*), main configuration and CI coefficient of the S_1 excited state calculated by TD-DFT//B3LYP/6-31+G(d,p) for compounds **3-6** based on the DFT//B3LYP/6-31+G(d,p) optimized ground state geometries.

Com-pound	Electronic Transition	TD-DFT/B3LYP/6-31+G(d,p)			
		Energy (eV)	*f*	Main Configurations	CI coefficients
3	$S_0 \rightarrow S_1$	2.68 eV, 463 nm	0.1265	HOMO→LUMO	0.6992
4	$S_0 \rightarrow S_1$	2.60 eV, 477 nm	0.1800	HOMO→LUMO	0.7010
5	$S_0 \rightarrow S_1$	2.67 eV, 462 nm	0.1343	HOMO→LUMO	0.6995
6	$S_0 \rightarrow S_1$	2.61 eV, 475 nm	0.2120	HOMO→LUMO	0.7017

Part IV: Mass Spectrum Studies

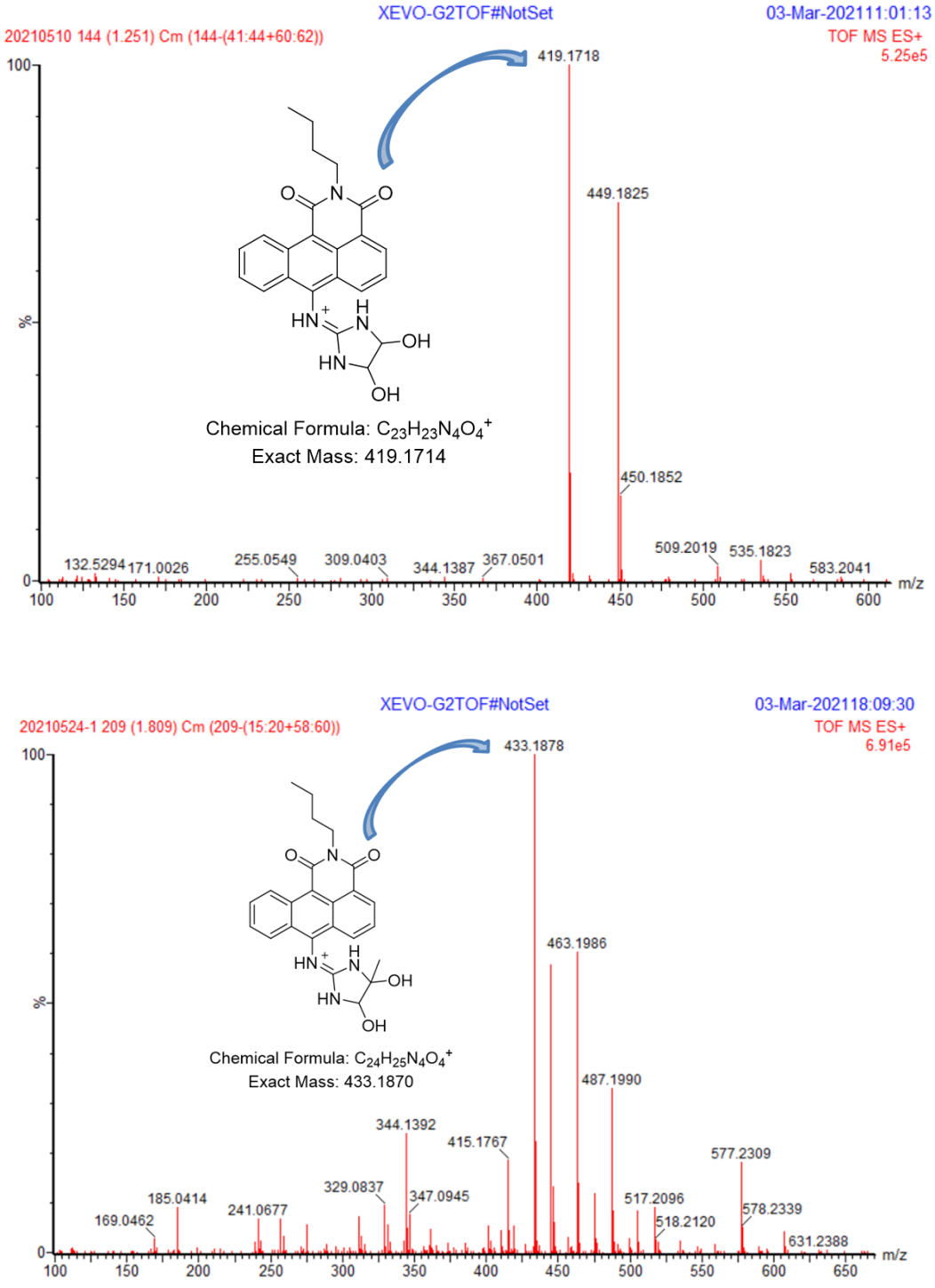

Figure S11 top: ESI-HRMS spectrum of the reaction mixture of **ANC-DCP-1** and **GO**. Below: ESI-HRMS spectrum of the reaction mixture of **ANC-DCP-1** and **MGO**.

Part V: GOS Level Detections in Urine Samples

5.1 Concentration-dependent fluorescence emission studies of ANC-DCP-1 upon incubation with 200 equiv. FA in a normal urine specimen.

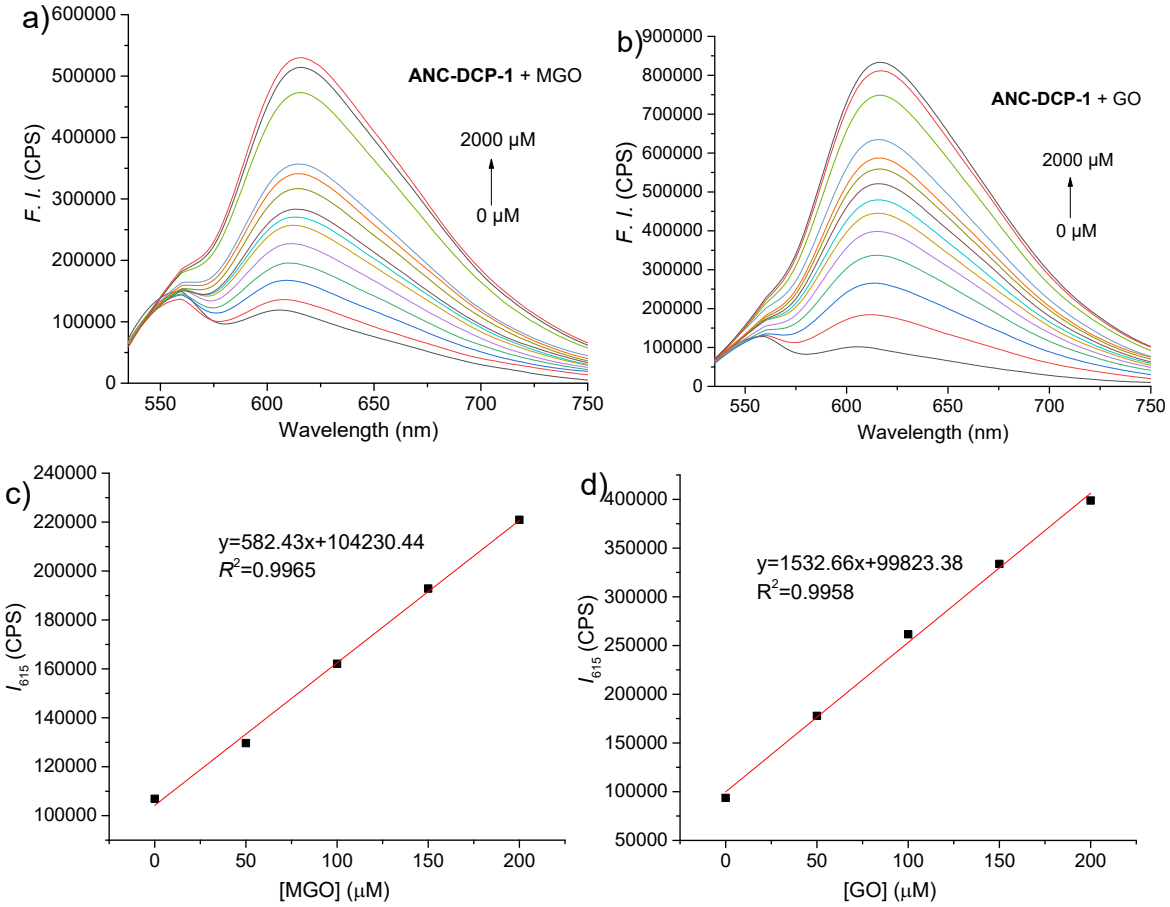

Figure S12 a-b) Concentration-dependent fluorescence emission spectra (λ_{ex}=525 nm) of the probe **ANC-DCP-1** (5 μM) in a normal urine sample (pH=5.9) incubated with 0-400 equiv. (0，25，50，100，150，200，250，300，350，400，450，500，1000，1500，2000 μM) MGO (a) or GO (b) at 37 °C for 2 h; c-d) Linear regression of fluorescence intensity at 615 nm (λ_{ex}=525 nm) of the probe **ANC-DCP-1** (5 μM) in a normal urine sample (pH=5.9) versus the concentrations (0, 25, 50, 100, 150, 200 μM) of MGO incubated for 1 h (c) or (0, 25, 50, 100, 150, 200 μM) GO (d) incubated for 2h. The detection limit (S/N=3) were calculated as 7.3 and 4.7 μM for MGO and GO respectively.

5.2 Patient recruitment and sample collection.

Five diabetic patient urine samples were collected at the Medical Laboratory Department of Hua Shan Hospital North affiliated with Fudan University with written informed consent obtained from the patients. The study protocol was approved by the Institutional Review Board of Hua Shan Hospital North, and the identities (except the individual age and gender) of the patients were kept confidential to the researchers at East China University of Science and Technology (ECUST). The urine samples were kept at 4 ˚C in a refrigerating box and assayed immediately upon receiving at ECUST.

5.3 GOS Detection in diabetic urine samples

The pH of all urine samples was adjusted to pH 6.0 by 1 M HCl or 1 M NaOH before addition of the probe **ANC-DCP-1** to a final concentration of 10 μM. The fluorescence intensity at 615 nm (λ_{ex} = 525 nm) was measured immediately after the probe addition. The urine sample with added probe were further incubated at 37°C, and then the fluorescence intensity at 615 nm was measured again. The results of normal urine samples and diabetic urine samples were shown in Table S2 and Table S3, respectively.

Table S2 Measured fluorescence intensity at 615 nm before and after incubation with 10 μM **ANC-DCP-1** for 2 h at 37 °C for normal urine samples

Normal urine sample No.	Fluorescence intensity at 0 min (CPS)	Fluorescence intensity at 120 min (CPS)	Fluorescence intensity increase (CPS)
1	58800.39	65326.64	6526.25
2	53485.63	63246.63	9761.00
3 (chylous)	79032.99	83928.30	4895.31
4 (chylous)	57939.27	59684.42	1745.15
5	55597.72	58103.53	2505.81

Table S3 Measured fluorescence intensity at 615 nm before and after incubation with 10 μM **ANC-DCP-1** for 2 h at 37 °C for diabetic urine samples

Normal urine sample No.	Fluorescence intensity at 0 min (CPS)	Fluorescence intensity at 120 min (CPS)	Fluorescence intensity increase (CPS)
1	62345.51	143820.74	81475.23
2	59937.15	107219.21	47282.06
3	75060.33	535602.43	460542.10
4	76404.22	983596.54	907192.32
5	56581.41	127156.71	70575.30

5.4 Examination of the glucose levels in the patients

The examinations of the patient glucose levels were conducted following the SOP of the Medical Laboratory Department of Hua Shan Hospital North affiliated with Fudan University (ISO15189 certified). The glucose levels of patients were measured by the hexokinase catalysis method on a Roche Cobas C automated biochemistry analyzer. The hexokinase catalyzes the phosphorylation of glucose to glucose-6phosphate (G-6-P) by ATP, and G-6-P can be oxidized by dehydrogenase in the presence of NADP. The detection method measured the concentration of glucose by monitoring the rate of NADPH formation. The patient blood samples were collected from a vein located on the inside of the elbow with a BD Preset 0.7 × 25 mm needle into a BD Vacutainer tube with 5 mg sodium fluoride and 4 mg potassium oxalate. After a brief centrifugation at 300 ×*g* for 3 min, the tubes were loaded on a Roche Cobas C analyzer to measure the glucose levels in the patient blood samples. The results were shown in Table S4.

Table S4 Blood glucose levels of the diabetic patients in the study

diabetic blood sample No.	gender	age	blood glucose level (mM)	
1	male	62	18.9	
2	male	57	17.5	
3	male	51	27.6	chylous urine
4	male	49	28.6	chylous urine
5	female	65	14.6	

Part VI: GOS Detection in Honey Samples

6.1 Fluorescence emission studies of ANC-DCP-1 in response to externally added MGO in diluted acacia honey.

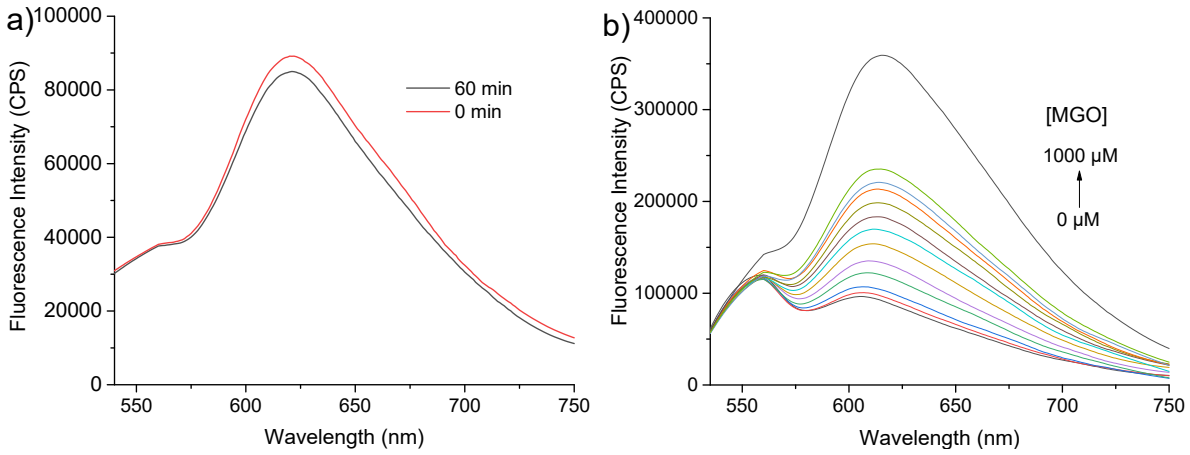

Figure S13 a) Fluorescence spectra (λ_{ex}=525 nm) of the probe **ANC-DCP-1** (5 μM) in diluted acacia honey (a mixture of 1 g acacia honey and 9 g pH 6.5 PBS solution) before and after incubation at 37

°C for 1 h; b) Concentration dependent fluorescence spectra (λ_{ex}=525 nm) of the probe **ANC-DCP-1** (5 μM) in diluted acacia honey (a mixture of 1 g acacia honey and 9 g pH 6.5 PBS solution) after incubation with various concentration of MGO (0-1000 μM) for 1 h.

Part VII: NMR and HRMS Data

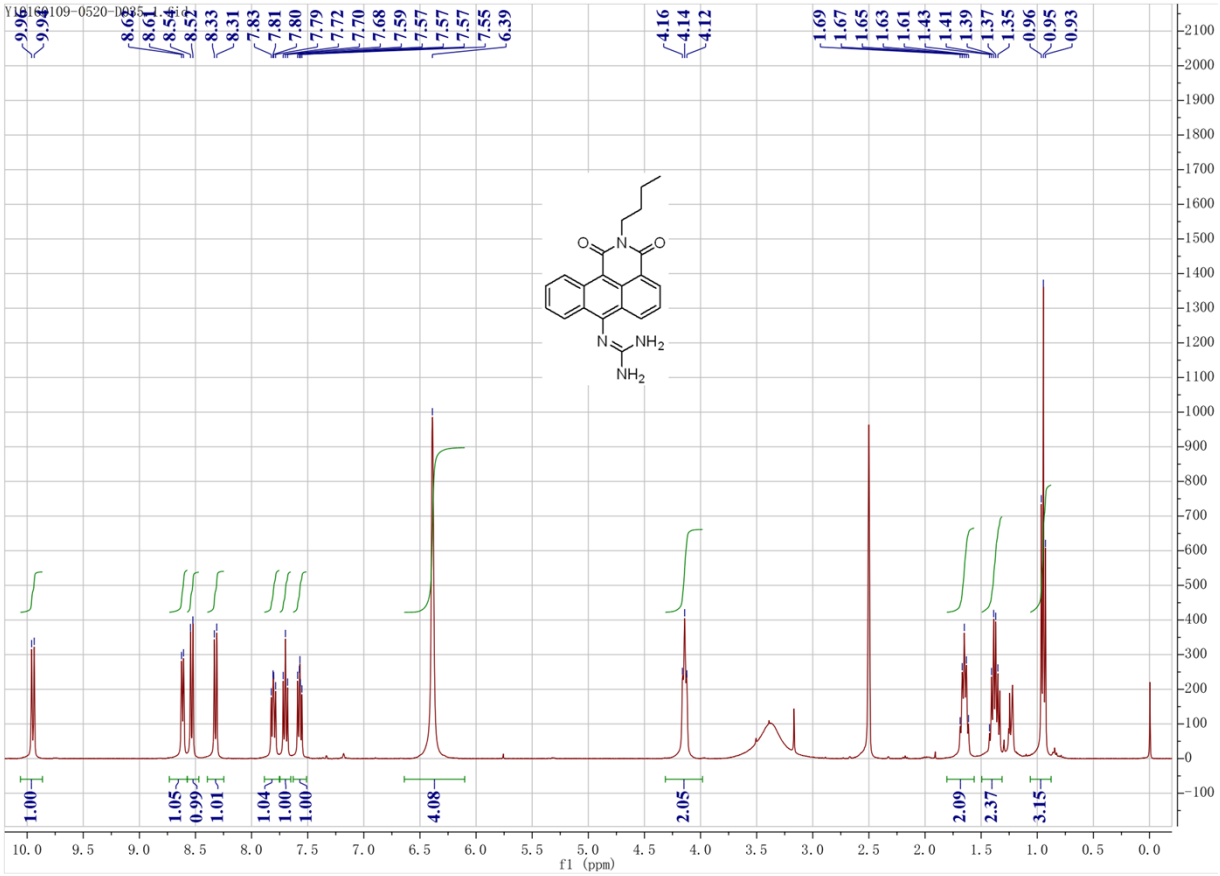

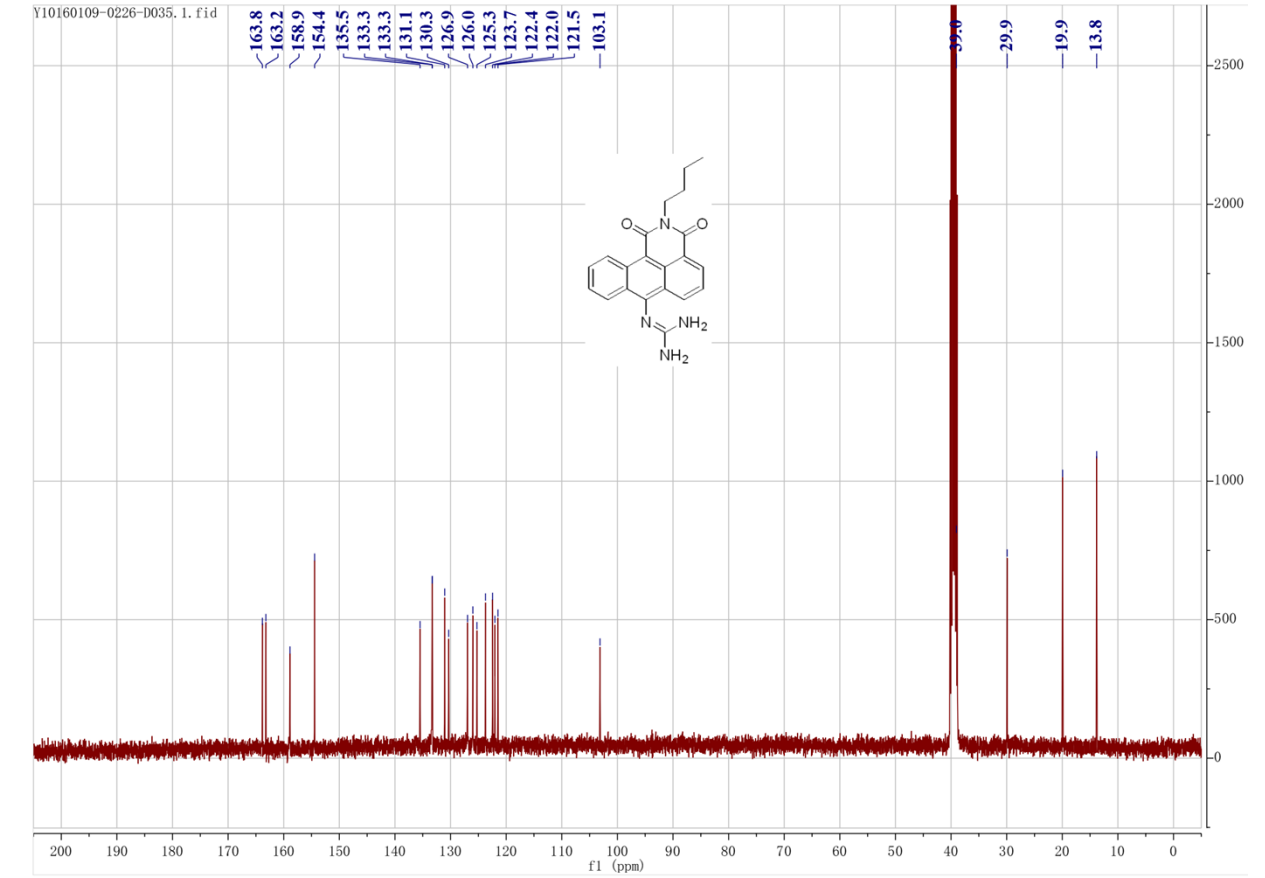

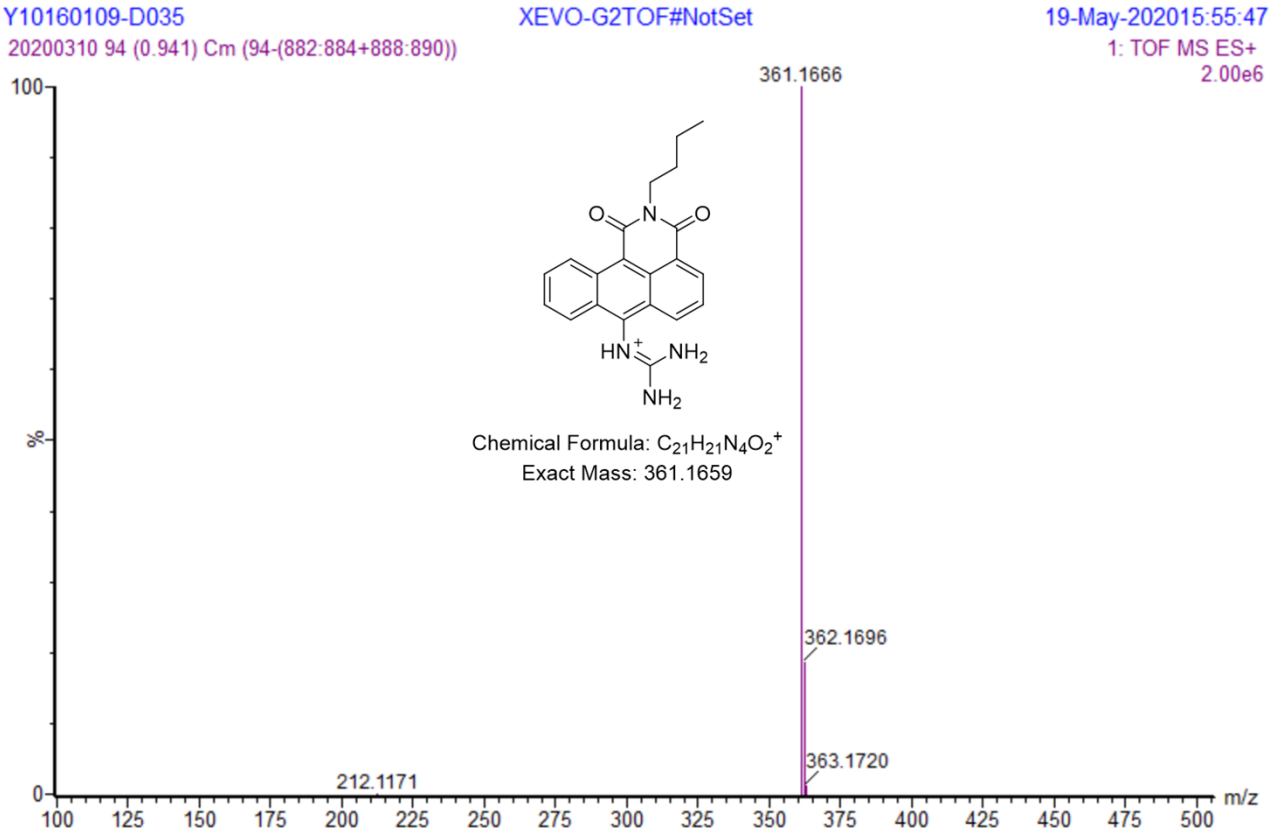

Figure S14 ^{1}H NMR, ^{13}C NMR, and HRMS of the probe **ANC-DCP-1**

References

1. Z. Gao, B. Han, K. Chen, J. Sun and X. Hou, *Chem. Commun.*, 2017, **53**, 6231-6234.
2. M. J. Frisch, G. W. Trucks, H. B. Schlegel, G. E. Scuseria, M. A. Robb, J. R. Cheeseman, G. Scalmani, V. Barone, B. Mennucci, G. A. Petersson, H. Nakatsuji, M. Caricato, X. Li, H. P. Hratchian, A. F. Izmaylov, J. Bloino, G. Zheng, J. L. Sonnenberg, M. Hada, M. Ehara, K. Toyota, R. Fukuda, J. Hasegawa, M. Ishida, T. Nakajima, Y. Honda, O. Kitao, H. Nakai, T. Vreven, J. A. Montgomery Jr., J. E. Peralta, F. Ogliaro, M. J. Bearpark, J. Heyd, E. N. Brothers, K. N. Kudin, V. N. Staroverov, R. Kobayashi, J. Normand, K. Raghavachari, A. P. Rendell, J. C. Burant, S. S. Iyengar, J. Tomasi, M. Cossi, N. Rega, N. J. Millam, M. Klene, J. E. Knox, J. B. Cross, V. Bakken, C. Adamo, J. Jaramillo, R. Gomperts, R. E. Stratmann, O. Yazyev, A. J. Austin, R. Cammi, C. Pomelli, J. W. Ochterski, R. L. Martin, K. Morokuma, V. G. Zakrzewski, G. A. Voth, P. Salvador, J. J. Dannenberg, S. Dapprich, A. D. Daniels, Ö. Farkas, J. B. Foresman, J. V. Ortiz, J. Cioslowski and D. J. Fox, *Gaussian 09*, Gaussian, Inc., Wallingford, CT, USA, 2009.